



Contact Lens Based Drug Delivery to the Posterior Segment Via Iontophoresis in Cadaver Rabbit Eyes

Keith Christopher¹ · Anuj Chauhan¹

Received: 24 October 2018 / Accepted: 7 April 2019 / Published online: 19 April 2019
© Springer Science+Business Media, LLC, part of Springer Nature 2019

ABSTRACT

Purpose A drug loaded contact lens combined with electrodes positioned diametrically opposite and beyond the limbus can potentially deliver ionic drugs directly to the vitreous.

Methods Commercial lenses are loaded with Nile blue or fluorescein as the drug analogs and placed on cadaver rabbit eyes. Electrodes (19.6 mm²) are placed atop at opposite sides of the sclera to apply a constant current (0.125–0.250 mA) for 1–2 h. COMSOL simulations are conducted to determine the field distribution and the potential drop across various tissue layers and equivalent circuit model is developed to calculate the electrophoretic velocity and estimate the drug flux.

Results The device delivered both hydrophobic and hydrophilic dyes to the tissue. The amount of fluorescein delivered to the vitreous directly correlated with the applied current and time duration. The electrophoretic mobility from the experimental data agreed with the model estimates. Confocal microscopy showed that Nile blue penetrated through the conjunctiva-sclera barrier to reach the retina showing that the electric field can transport molecules through the ocular tissue and into the vitreous. The ex vivo model neglects transport into flowing capillaries in the choroid. However, the time scale for electrophoretic transport across the choroid was found to be 550–1300 fold shorter than that for uptake into the choroidal capillaries.

Conclusion Incorporation of an electric field with multiple electrodes on a single lens can effectively deliver ionic drugs to the posterior region at levels comparable to current methods with the benefits of being safer and less invasive.

KEY WORDS contact lenses · COMSOL · drug delivery · ex vivo · iontophoresis

ABBREVIATIONS

HEMA Hydroxyethylmethacrylate
PBS Phosphate buffered saline
HEPES (4-(2-hydroxyethyl)-1-piperazineethanesulfonic acid)

INTRODUCTION

Recent pharmacological advances have produced therapeutic treatments for some common and severe afflictions originating in the posterior eye segment (1–7). For example, macular edema or diabetic retinopathy can be treated using a vascular endothelial growth factor (VEGF) inhibitor to prevent the overexpression of VEGF which can also lead to increased cancer growth and metastasis (8). The inhibition of VEGF can also slow the progression of age-related macular degeneration (AMD), which affects over 1–3% of people over the age of 50 every year (9). Once a patient has AMD, the anti-VEGF treatment requires up to 8 vitreal injections over the course of a year due to the drug being cleared from the area within several days (10). Even though the injections allow for nearly instantaneous drug activity to the afflicted area with a significant bioavailability, the process is accompanied by numerous potential complications. The most notable are endophthalmitis, retinal detachment, hemorrhages, infections, severe irritation, and general toxicity concerns (11).

As a result of these potential problems, there has been significant work into developing new methods for the delivery of therapeutics to the posterior eye segment. Some of the more appealing developments are microspheres or nanoparticles for increased retention and prolonged release, injectable and slow release devices, and sclera implants (12–14). All of these new

✉ Anuj Chauhan
chauhan@che.ufl.edu

Keith Christopher
chri5099@ufl.edu

¹ Department of Chemical Engineering, University of Florida
1030 Center Drive, Gainesville, Florida 32611, USA

technologies offer their own beneficial qualities, mainly aimed at the prolonged release to minimize the number of follow up visits and treatments. However, they all still require invasive approaches such as direct injection into the vitreous or another form of surgical implantation.

One of the promising concept for the non-invasive delivery of therapeutics is possibly iontophoresis, which utilizes electromotive forces to deliver charged molecules using an electric field and drives the species of interest through barriers with low permeabilities (15). Recently, the technology has been sought after for ophthalmic applications (16,17). For example, the Eyegate is a compact device with an electrode adjacent to a drug reservoir that is placed over the eye while a counter electrode is attached to the forehead or earlobe (18). The device supplies a safe amount of current that carries a drug from the reservoir and into the eye and through the dense cellular layers that hinder the free diffusion of drugs into the eye. Another possible advantage of this technology is the non-invasive delivery of much larger molecules such as oligonucleotides which carry significant charge (16). However, some disadvantages of using these devices are that they are typically quite bulky and require a patient to keep their eye open for an extend period of time and only target the front of the eye or the sclera. However, the concept of iontophoresis seems to show great promise for the non-invasive delivery of therapeutics to the posterior eye segment.

Some of the limitations of the iontophoretic devices can be mitigated by designing more user friendly platforms such as contact lenses containing both electrodes – cathode & anode, alleviating the need for attaching the counter electrode to ear or forehead, which makes the device bulky. If both electrodes and the power source are placed on the same lens, a patient could possibly close their eyes while the system is worn, which can improve comfort during use allowing for longer wear duration, at a lower and safer current density. However, attaching both electrodes to the lens could lead to significant current flow short-circuiting through the lens which could reduce the efficacy of the drug delivery. Here we focus on testing a novel configuration using a contact lens that extends past the cornea where the electrodes are located diametrically opposite and over the sclera. It is hypothesized that the applied field will pass almost entirely through the sclera, choroid, retina, and vitreous leading to rapid transport into the vitreous or potentially to the retina and choroid depending on the duration of field application and physical properties of the drug including charge, diffusivity, electrophoretic mobility and partition coefficients in various ocular tissues. The proof of concept experiments explored here focus on showing that fluorescent charged molecules can be delivered to the retina and/or vitreous by application of field in an ex vivo model of rabbit eyes. Other critical issues that were explored were that of osmotic swelling or shrinking of the eye tissue near the electrodes and the electrodic reactions that generate gases

and caustic species. Our results support the possibility for the delivery of therapeutics to the posterior eye segment through iontophoresis in significant quantities.

METHODS

Materials

Mature cadaver albino rabbit eyes were purchased from Pel-Freez Biologicals (Rogers, AR). The Nile blue A dye (75% dye content, MW: 354 g/mol, net charge: +1) and fluorescein (MW: 332 g/mol, net charge: -1) were purchased from Sigma-Aldrich (St. Louis, MO). Electrode materials were made 3D printed with conductive PLA filament (Proto Pasta, Vancouver, WA). Cadaver rabbit eyes were fixed in Margo solution containing paraformaldehyde and glutaraldehyde purchased from Fisher Scientific (Hampton, NH). Soaking agents for lenses included phosphate buffered saline (PBS) or a HEPES solution purchased from Fisher Scientific (Hampton, NH). Commercial contact lenses Acuvue Oasys (14 mm diameter, 8.4 mm base curve, 0.0 power) were used in the study.

Lens Preparation

Contact lenses were loaded by soaking in a 1 mg/mL Nile blue solution in PBS overnight and has a partition coefficient of roughly 30 in Acuvue Oasys lenses and results in roughly 400 µg in the lens after loading. For fluorescein loading, lenses were loaded with a 0.10 mg/mL fluorescein solution in HEPES overnight and has a partition coefficient of 4 in Acuvue Oasys lenses and yields roughly 26 µg of fluorescein in the lens. Lenses were loaded overnight in an enclosed space to ensure concentrations in the lenses were consistent and to prevent photobleaching of any species. Additionally, lenses without dyes or drugs for the counter electrodes were soaked for 10 min in PBS (if applied to the anode) or HEPES (if applied to the cathode). Both dyes are low molecular weight compounds and therefore have rapid uptakes into the lenses.

Application of Electric Field

Commercial contact lenses used here were not large enough to extend sufficiently beyond the limbus. Therefore, the loaded contact lenses were cut into two equal parts and placed diametrically opposite at the periphery of the cornea, i.e., on the sclera, and the two electrodes were gently rested against the lenses to ensure the electrodes were completely in contact with the surface. The electrodes were 3D printed with a conductive PLA filament and had a cross-sectional area of 19.6 mm². Many researchers have integrated electrodes and a power supply onto contact lenses (19,20) but here, for

simplicity, electrodes were attached to an external power source that was set to the desired current (Fig. 1). A syringe pump was configured to gently apply a drop of PBS ($\approx 30 \mu\text{L}$) every 3 min on to the lenses for the delivery of fluorescein and for Nile blue a drop was applied every 30 s, providing a thin film to keep them hydrated. The application of PBS also served as an approximate mimic of the *in vivo* tear film. Although the flow rate is higher than what is typically seen *in vivo*, the excessive PBS ran off while the residual amount left after drop application was small enough to assume the similarity to the tear film volume. The submersion of the lens was also crucial to ensure that if any bubbling from electrochemically generated gases were to occur, it would be easily visible (21). The field was applied for the desired duration and then the power source and lenses were removed. Experiments were conducted with the lenses soaked in PBS for the anode and HEPES for the cathode. The Nile blue and fluorescein experiments were each conducted with three different combinations of time and current.

Imaging Via Confocal Fluorescent Microscopy

The imaging of Nile blue was done for all three combinations of time and current at both the anode and cathode. For the control, which was the placement of a lens for 1 h on the eye without an electric field, only a single image of the eye was taken at the spot adjacent to where the lens was placed. Nile blue excitation and emission occurs around 630 nm and 665 nm respectively. This makes it ideal for confocal microscopy in the far-red region. The preparation of the cadaver rabbit eyes after Nile blue delivery was first done by fixation in Margo formulation. The fixative solution consists of 1% paraformaldehyde and 1.25% glutaraldehyde in PBS and the whole eyes were submerged for 40 h. After fixation, the eyes were cross-sectioned to include both regions that were adjacent to each electrode and put in a glass bottom dish filled with PBS. The dishes were mounted on a Nikon A1 laser scanning confocal microscope to observe the distribution of

the Nile blue in the regions adjacent to the electrodes. All images were captured and processed with identical imaging properties.

Fluorescent Quantification of Fluorescein Delivery

Delivery of fluorescein to the posterior eye segment was conducted three times for each variation of time and current and a control for the case with passive diffusion was conducted where the lens was placed on the eye for 1 h without the electric field. After completion, the vitreous was immediately harvested and centrifuged to remove any residual tissue. Each sample was individually measured for relative fluorescent intensity using a Quantech fluorometer and the corresponding concentrations of fluorescein was found through a calibration curve.

Model

A simplified 2D model was simulated using COMSOL to determine the distribution of the electric field through the eye with electrodes in a spot (Fig. 2a) and concentric (Fig. 2b) configuration. The geometries include a contact lens with electrodes adjacent to the drug loaded contact lens and the whole eye. The geometries also incorporated all layers of the posterior eye segment, lens, cornea, and ciliary body with properties obtained from literature (Table I). The current density from the anode was fixed at a value equivalent to $0.5 \text{ mA}/\text{cm}^2$ which is a physiologically safe value for current density in ocular tissue, although higher values have been used for ocular iontophoresis (22,23). The distribution of the electric field, which follows Laplace's equation for potential distribution ($\nabla^2\phi = 0$), with a fixed current density at anode and zero potential at the cathode. Zero flux at the remaining boundary and continuity of current across all other boundaries were imposed as boundary conditions. The Laplace equation for potential distribution was solved using the 'AC/DC' module in COMSOL to determine the electric field distribution.

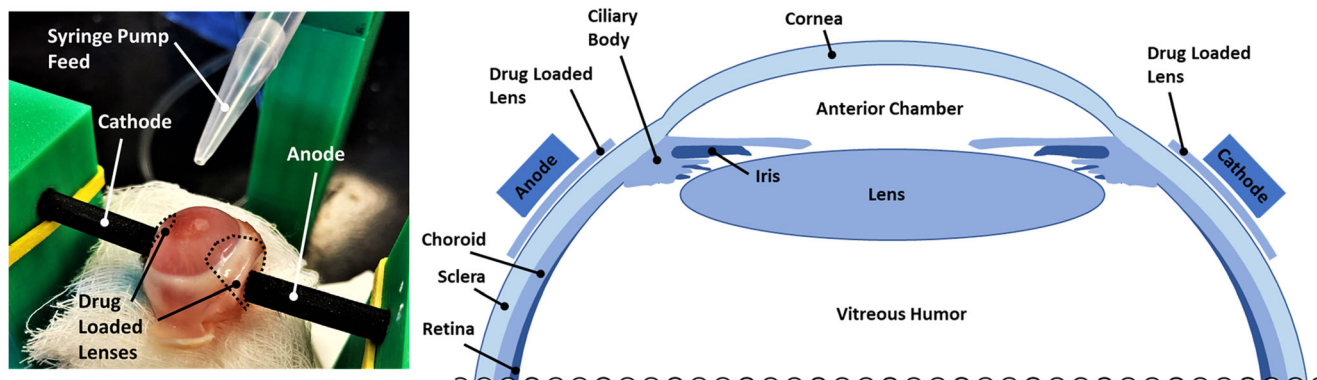


Fig. 1 Ex vivo arrangement of drug loaded contact lenses and spot electrode configuration on cadaver rabbit eyes. The electrodes are placed on opposite sides of the sclera just below the site of the ciliary body and muscle and are connected to a constant current power source. The electrodes rested atop the drug loaded contact lenses while a syringe pump supplied a steady droplet system to prevent the lenses from drying out.

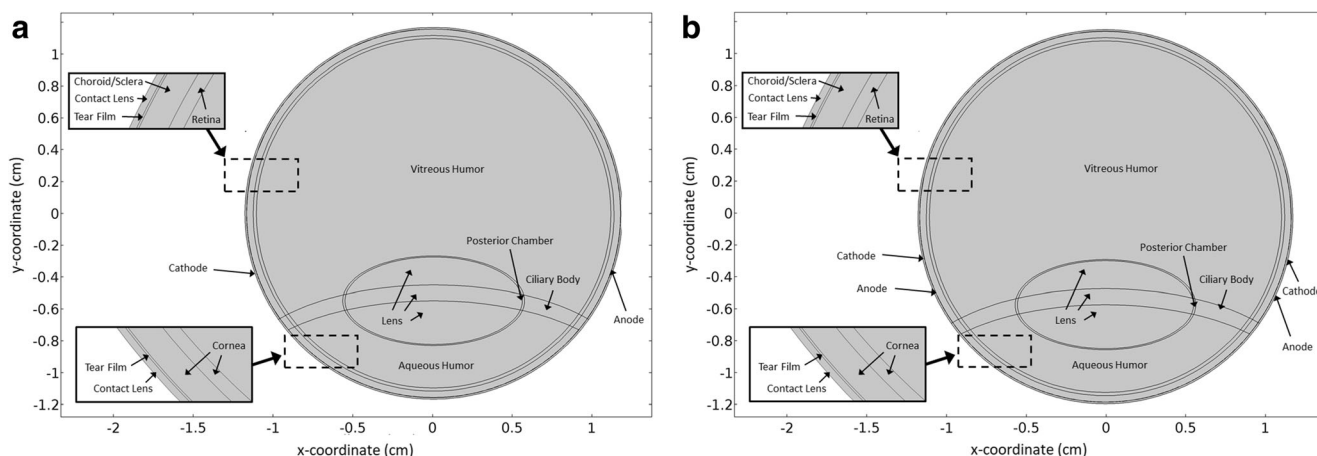


Fig. 2 COMSOL representation of an eye and scleral lens with surface electrodes. The geometry of a simplified human eye with a contact lens and electrodes to provide an electric field. The enlarged sections depict the geometry and material in the posterior and anterior segments of the eye. **(a)** spot electrode configuration, **(b)** concentric electrode configuration.

RESULTS

Nile Blue Delivery

In order to visualize the concentration profile of drugs as they are delivered through the sclera, choroid, and retina, confocal microscopy of cadaver rabbit eyes was employed with nile blue loaded contact lenses after the application of the electric field at different strengths (high current: 0.25 mA, low current: 0.125 mA) and durations (short time: 1 h, long time: 2 h) (Fig. 3). The pH of the lenses was held around 7.6 by the PBS, rendering nile blue ($pK_a = 9.5$) almost entirely ionized, resulting in the maximum iontophoretic transport possible (24). It is clear from the images that even at a low current and a short time duration, there was sufficient transport of nile blue across all layers and into the retina. It is difficult to clearly discern the boundaries between various tissues but it appears that the nile blue concentration is high in conjunctiva and retina, and low in choroid. It is worth noting that nile blue has a very low diffusivity through tissue due to its selective binding to DNA. The presence of nile blue in the retina

suggests that the transport of the dye was sufficiently rapid to at least traverse the entire conjunctiva-sclera-choroid-retina pigment epithelium- retina. In contrast to the control which was conducted by placing a lens on the eye and allowing the nile blue to passively diffuse for an hour. The control revealed no nile blue in any region of the posterior eye segment, illustrating that the electric field significantly increases the transport of nile blue through the posterior eye segment.

Fluorescein Delivery

The fluorescein was loaded into lenses in a HEPES solution, which minimizes the potential for damage done to the eye during the generation of caustic species from the electrochemical reactions and holds the pH at a value that renders the fluorescein almost entirely ionized to maximize iontophoretic transport. To quantify the delivery of fluorescein to the posterior eye segment, experiments were conducted at the three different combinations of time and current, the same that were used for the delivery of nile blue and were compared to a control which consisted of a lens applied to the eye for

Table 1 Values used in the COMSOL Model, Equivalent Circuit Model, and Electrophoretic Velocity Analysis

Region	Thickness (μm)	Resistivity ($\Omega \cdot \text{cm}$)	Relative Permittivity
Contact lens	100	25,000	130
Tear film (35,36)	10	78	78
Sclera and choroid (36,37)	400	2700	150,000
Retina (36,37)	200	4000	150,000
Vitreous humor (35,36)	11,000	78	78
Aqueous humor (35,36)	–	78	78
Cornea (35)	600	10^6	10^4
Lens (35)	–	10^5	10^4
Ciliary body and iris (38)	–	3500	10^4

1 h without electric field. After the application of the electric field to the sclera, the vitreous was harvested and fluorescence was quantified using a fluorometer instead of employing the confocal microscopy method used to visualize Nile blue. This was done because fluorescein is very hydrophilic and is expected to accumulate in the vitreous instead of the tissue. The concentrations of fluorescein were found using a calibration curve for the relative fluorescence (Table II). Additionally, in Fig. 4, the delivery and localization of fluorescein can be seen visually in the posterior eye segment after fluorescing the dye via a UV light source and imaging through an orange filter. The regions near the cathode show localizations of fluorescein at the exterior and interior surfaces. The final concentration in

the vitreous was also used to calculate the time averaged flux of the fluorescein and the electrophoretic velocity.

COMSOL

A simplified 2D model was constructed to explore the current distribution and determine the optimal electrode placement. The model was simplified to a 2D geometry to decrease the computational load but still provides a solid basis for the intended purposes. For the COMSOL model with the spot electrode configuration, the current density from one electrode was fixed at a value equivalent to 0.5 mA/cm^2 which is a physiologically safe value for current density in ocular

Fig. 3 Confocal images of cross-sectioned cadaver rabbit eyes after iontophoretic delivery of Nile blue. The distribution of Nile blue (red) at various currents and field application times at regions adjacent to the cathode, anode, and control case with purely passive diffusion from a drug loaded lens. In the control case, the diffusive resistance was too high and did not penetrate the ocular tissue. No Nile blue was visible near the cathode due to Nile blue being a cathodic dye. Adjacent to the anode, Nile blue penetrates into the retina. It is difficult to clearly discern the boundaries between various tissues but it appears that the Nile blue concentration is high in conjunctiva and retina, and low in choroid. Tissues are labeled in the anode images (Conjunctiva (Cn), Choroid (Ch), Retina (R)) (scale bar: $250 \mu\text{m}$).

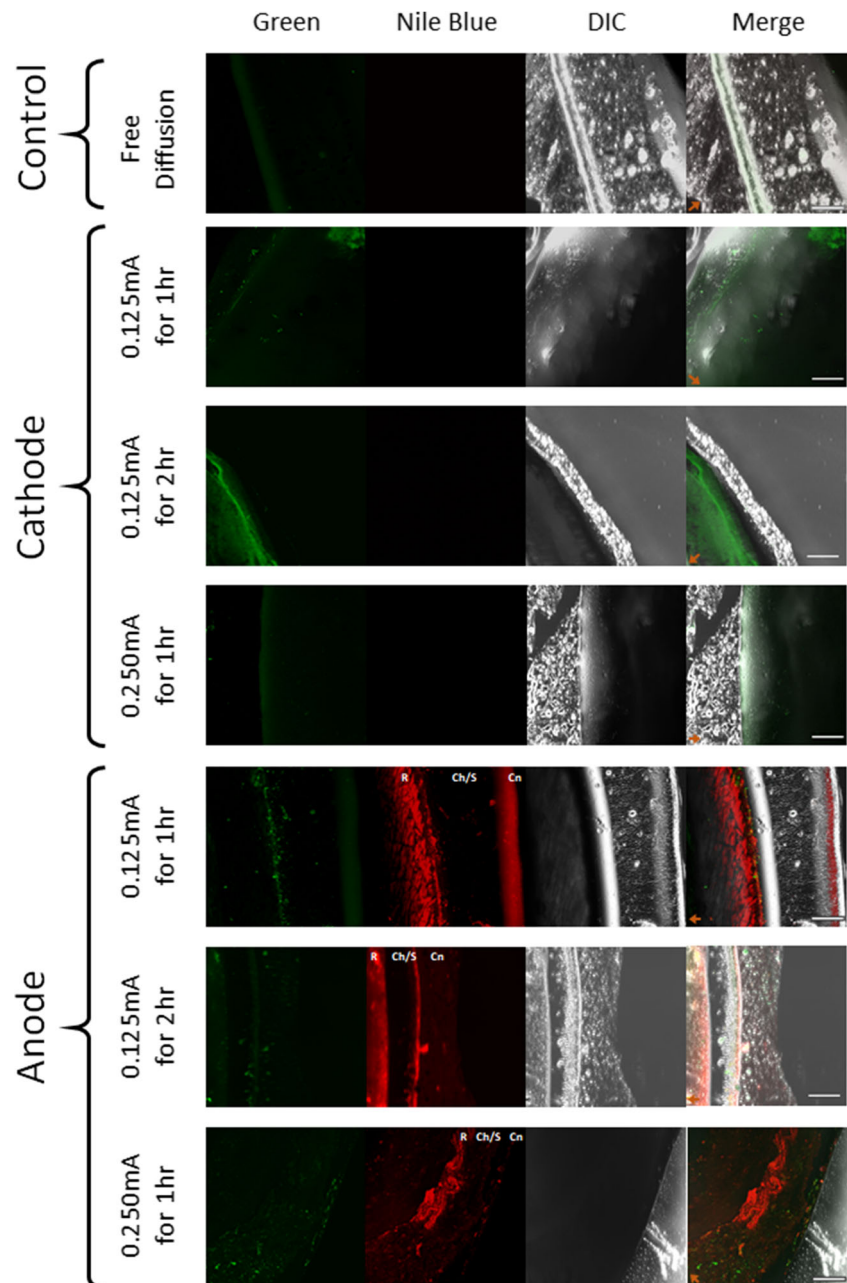


Table II Concentration of Fluorescein in the Vitreous which was used to Calculate the Experimentally Observed Flux and Electrophoretic Velocity

	Fluorescein in Vitreous (μg)	Flux ($\mu\text{g}/\text{m}^2\text{s}$)	Electrophoretic Velocity ($\mu\text{m}/\text{s}$)
Control	N/A	N/A	N/A
1 h 0.250 mA	2.17 ± 0.34	6.68 ± 0.65	1.34 ± 0.07
2 h 0.125 mA	3.15 ± 0.74	4.86 ± 1.15	0.97 ± 0.23
1 h 0.125 mA	1.80 ± 0.21	5.54 ± 1.04	0.55 ± 0.21

tissue, while the potential is fixed to zero at the counter electrode. The distribution of the electric field, which follows Laplace's equation for potential distribution ($\nabla^2\phi = 0$), shows a majority of the potential drop is through the contact lens and partially through the sclera and choroid (Fig. 5). Additionally, the streamlines indicate the flow of current between the electrodes and that nearly all current penetrates the vitreous humor with only a small amount of current passing through the posterior chamber and aqueous humor. Furthermore, the negligible voltage drop through the retina and vitreous shows that once the drug of interest reaches the retina, the electric field will have much less of an effect on migration. Essentially meaning that once the drug reaches these areas, it will be more prone to free diffusion into the surrounding solution rather than following the electric field in its entirety to the counter electrode. The model also shows that the maximum

safe current density can be achieved with a relatively low electric potential gradient.

In the model with concentric electrodes, the same value for current density was used to maintain physiological relevance and for direct comparison between the models. The distribution of the electric field shows a majority of the current passing through tissue and into the vitreous (Fig. 6). Some also passes directly through the sclera/choroid and then returns to the counter electrode without penetrating the retina. The areas of greatest voltage drop are the contact lens and the sclera/choroid while there is a somewhat lesser effect in the retina but still shows a moderate amount of potential drop. However, the potential drop in the sclera/choroid is both directly towards the vitreous and lateral, demonstrating that the concentric arrangement can be useful for targeted drug delivery to the choroidal space. However, since the spot electrode

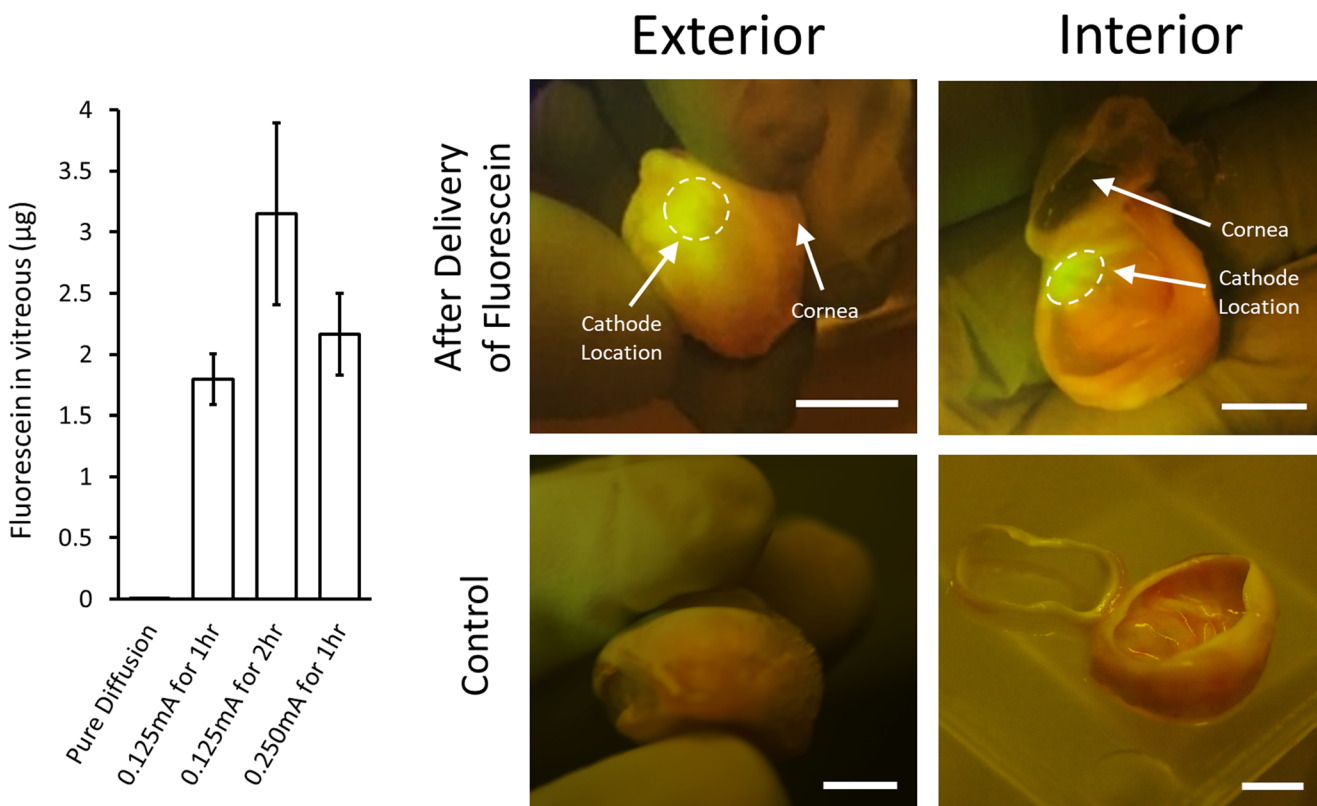
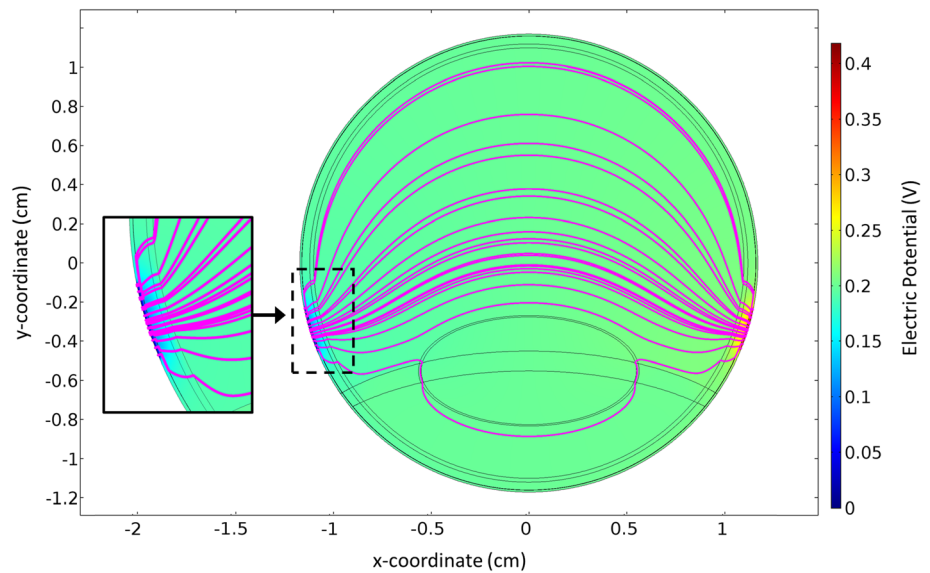


Fig. 4 Quantification of fluorescein in posterior eye segment. Graph indicates the total amount of fluorescein that was delivered to the vitreous humor after application of corresponding electric fields ($n = 3$). Images taken with Nikon D810 camera with blue light source and orange filter exhibits the presence of fluorescein throughout the tissue in the posterior eye segment at the region near the cathode and control eyes do not display any fluorescence without any fluorescein present. (scale bars: 5 mm).

Fig. 5 Electric potential distribution through the eye with the spot electrode arrangement. The simplified representation of the eye with spot electrodes on either side of the sclera. The voltage drop can be seen to primarily take place through the contact lens and the sclera/choroid region. The streamlines indicate the path of the current, which predominantly passes through the vitreous with a small degree of current passing through the posterior chamber and into the aqueous humor.



arrangement shows a greater deal of current penetrating the vitreous, this was the design explored in the ex vivo models.

Equivalent Circuit Model

An equivalent circuit model of the contact lens and the posterior eye segment was constructed to obtain simplified expressions for the strength of electric field in various tissues, which places all the layers in series. The results of the COMSOL model indicate that nearly all of the current passes through the posterior eye segment without short circuiting through the contact lens or the tear film when the electrodes are in the spot configuration. The circuit equivalent model can be used to estimate the efficacy of the drug transport and assist in illustrating areas of greatest potential drop which are the regions where the drug will be most influenced by the electric

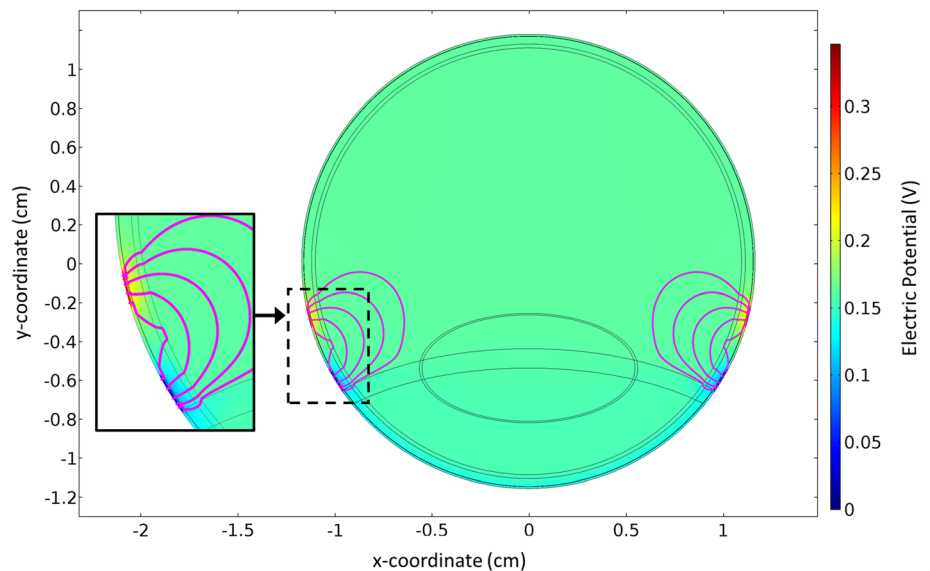
field and assist in deriving the expressions for the electrophoretic velocity.

First, for each layer of the eye, the effective resistance (R_i) can be calculated by using the resistivity of a layer (ρ_i), the thickness of the layer (h_i), and the cross-sectional area that the field is passing through (A) which is found in Eq. 1 and each resistance can be found using the properties in Table I.

$$R_i = \frac{\rho_i h_i}{A} \quad (1)$$

After finding the resistance of each layer, the ratio of that layer to the total resistance represents the percentage of the voltage drop within that layer. Since the overall potential is known, the potential through a single layer can now be found for the calculation of the electrophoretic velocity. The areas used for the tissue layers was 1.5 times the area of the

Fig. 6 Electric potential distribution through the eye with the concentric electrodes. The simplified representation of the eye with concentric electrodes just behind the cornea and ciliary body. The voltage drop can be seen to primarily take place through the contact lens and the sclera/choroid region. The streamlines indicate the path of the current, which mostly passes into the vitreous before returning to the counter electrode with some passing only through the sclera/choroid region.



electrodes due to the high potential gradient through the tissue which yields field lines that take the shortest possible path, as seen in the COMSOL simulation. The area for the vitreous was roughly half the total cross-sectional area of the eye due to the spreading of the field lines once inside the vitreous chamber. Additionally, the potential drop in the capacitance double layer next to the electrode and the charge transfer resistance was neglected in this simplified model.

Using the equivalent circuit model and values from Table I, the resistances for each layer was calculated and the percentages of the total resistance were also found (Table III). These values were then compared to the potential drop in each layer of the eye, taken from the COMSOL model. Comparing the values, the relative percentages of the total resistances from the equivalent circuit model matches well with the percentages of the voltage drops from the COMSOL model with the only minor deviation of note is the vitreous. This can be attributed to the changing area through the vitreous as the field propagates to the counter electrode. However, the strong correlation between the equivalent circuit and COMSOL models validates the general approximations for the system that were assumed in constructing the equivalent circuit model.

Average Electrophoretic Velocity of Fluorescein through the Eye

The resulting concentrations of fluorescein in the vitreous can be used to calculate the time averaged electrophoretic velocity (v_{ep}) in Eq. 2 which is a function of the charge of the species (z), the diffusion coefficient of the species (D), the potential (V), and a characteristic length over the potential drop (ℓ).

$$v_{ep} = \frac{zeDV}{kT\ell} \quad (2)$$

In the sclera and choroid, fluorescein has a relatively high diffusion coefficient on the order of $100 \mu\text{m}^2/\text{s}$ to $10 \mu\text{m}^2/\text{s}$ (7,25,26). Using a diffusion coefficient of $50 \mu\text{m}^2/\text{s}$, the potential drop found through the COMSOL model, and the width of each layer as the characteristic length, the theoretical electrophoretic velocity was found through each layer (Table III). Using the experimental data from Table II, the

electrophoretic velocity was determined to be 0.55 and $1.34 \mu\text{m}/\text{s}$ for the low and high current experiments respectively. This agrees well with the calculated values for the theoretical electrophoretic velocity and averaged for the transport through all layers with a diffusivity of $50 \mu\text{m}^2/\text{s}$ (Table III) using Eq. 2. The difference can be accounted for the fluorescein that is still embedded in the tissue once the electric field has been terminated after the conclusion of the experiments. Additionally, the theoretical maximum distance covered with the applied current and time durations would only be 2–5 mm which is partially into the vitreous but not entirely through to the tissue adjacent to the counter electrode. This explains why there is no aggregation of fluorescein or Nile blue at the counter electrodes. Instead, the drugs remained within the vitreous rather than following the current to completion at the counter electrode. It should also be mentioned that since the electrophoretic velocity was time averaged and taken from the results of the fluorescein experiments, it considered all existing charged species in the ex vivo system rather than an isolated system where only the drug of interest carries current.

Additionally, the comparison of the electrophoretic velocity to the rate of uptake in choroidal capillaries will reveal if the delivery of the drug assisted with an electrophoretic driving force. This is significant because it has been suggested that the main reason that scleral implants have minimal drug delivery is due to the blood flow in the choroidal capillaries that takes up drug, preventing it from reaching the vitreous. However, in the ex vivo experiments, there is no blood flow, which will possibly yield significantly more drug than expected compared to an *in vivo* model. Therefore, comparing the expected rate of delivery to that of the uptake by the capillaries in the choroid will reveal if there will be any significant discrepancies between the ex vivo and theoretical *in vivo* models. The primary term for comparison is the time scale for transport into the blood vessels in the choroidal capillaries and that for electrophoretic driven transport across the vitreous. The time scale for transport into the capillaries depends on multiple factors including capillary density and permeability of the capillary walls to the solute. A detailed model for this transport is not developed here but many other researchers have integrated loss from the choroidal capillaries into generalized model for drug transport in the retina. Based on literature the inverse of

Table III Layer-by-Layer Calculations for the Theoretical Electrophoretic Velocity and Values for Potential Drop and Resistance Found in the COMSOL Model and Equivalent Circuit Model Respectively

Layer	Theoretical Electrophoretic Velocity ($\mu\text{m}/\text{s}$)	Potential Drop (V)	% Potential Drop	Resistance (Ω)	% Resistance
Contact Lens	2.222	0.115	57.5%	1275	57.0%
Choroid/Sclera	0.242	0.05	25.0%	550	24.7%
Retina	0.338	0.035	17.5%	407	18.3%
Vitreous	1.76×10^{-3}	0.01	5.0%	5×10^{-3}	–

the time scale for clearance through the choroidal circulation (β), which was found to be $1.98 \cdot 10^{-5} \text{ s}^{-1}$ for fluorescein (27). The time scale for electrophoretic transport across the choroid is the ratio of the choroid thickness and the electrophoretic velocity, which is estimated as discussed above. Proper scaling analysis shows that the appropriate expression for the electrophoretic transport is a function of the electrophoretic velocity (v_{ep}) found in Table II and the width of the choroid ($h = 200 \text{ }\mu\text{m}$) (Eq. 3).

$$\frac{l}{\beta} \sim \frac{h}{v_{ep}} \quad (3)$$

Direct comparison shows that the time scale for the electrophoretic transport at the lower and higher current is over 550 and 1300-fold lower than that of the time scale for loss to the choroidal circulation. This simple analysis suggests that the electric field driving the drug delivery is sufficient to overcome the losses to the choroid, and that absence of blood flow in the choroid in this *ex vivo* model has only a small impact on the final concentration in the vitreous. This result is however based on a simple scaling analysis, and must be further explored through more detailed mathematical models and *in vivo* studies.

For pure diffusion the time scale of transport across the choroid can be estimated as the square of the thickness of the choroid divided by the diffusivity. For a thickness of $200 \text{ }\mu\text{m}$ and diffusivity of $50 \text{ }\mu\text{m}^2/\text{s}$, this time is about 800 s, which is still shorter than the time scale for loss to the choroidal circulation and longer than that for the time scale for electrophoretic transport. This analysis suggests that the choroidal loss is not significant both for pure diffusion and electrophoretic transport, in agreement with prior publications (27). It should be noted though that the scaling analysis is a useful yet preliminary approach to compare rates for parallel processes such as transport into the vitreous and that into the choroidal circulation. A more detailed theoretical calculation along with *in vivo* animal experiments would be needed to draw firm conclusions regarding the fractional drug that can be cleared into the choroidal circulation.

DISCUSSION

Electric Field through Oversized Contact Lens Significantly Increases Drug Delivery through Posterior Eye Tissue

The delivery of drugs to the posterior segment of the eye cannot always be accomplished by passive diffusion, even if there is a concentrated source implanted at the base of the sclera (27). This is mostly due to the thickness of the sclera and retina along with the blood flow through the choroid which has one of the highest blood flow rates in the human body.

These factors result in the need for an additional driving force to enhance the transport of the drugs through the thick and dense tissue in the posterior eye segment. Therefore, the use of an electric field within the limits of physiological acceptability can provide adequate assistance. Here, we used cadaver rabbit eyes with drug loaded lenses and electrodes applied to opposite sides of the posterior region of the eye that supplied the electric field.

In the case of fluorescein, the amount delivered correlated with both the duration and strength of the applied electric field and no fluorescein was found in the vitreous in the control case which was pure diffusion from a lens for 1 h. The results show that increasing the current marginally increases the amount of fluorescein delivered and that doubling the time that the electric field is applied nearly doubles the amount of fluorescein in the vitreous. The control cases saw no fluorescein permeate into the vitreous which would take several hours to traverse the contact lens, sclera, choroid, and retina. This is expected due to the variations in flux and the electrophoretic velocity in regard to the applied field strength and the time scale of the experiments which is in agreement with previous works (28). That is why the cases with low current have similar fluxes and the case with high current has a higher flux, correlating with the strength of the applied electric field. All cases with iontophoresis have fluorescein present in the vitreous where the control case did not and demonstrates how the application of an electric current significantly increases the transport of species. Furthermore, the amount of fluorescein is several orders of magnitude higher than some intravitreal injections (29) and is on the order of typical therapeutic levels of some drugs that are injected into the vitreous (30). However, for drugs that may require higher concentrations, the loading concentration for the drug can be adjusted to increase the amount of drug in the lens or by adjusting the area of the electrodes. Although the comparison of other drugs with different properties may not be completely valid, it serves as a starting point for drugs with similar size and charge.

The distribution of Nile blue was uniform across all applied currents and times due to the high electrophoretic velocity that led to complete delivery across the sclera, choroid, and retina while the control case did not have any Nile blue permeate the tissue. This confirms that adequate delivery of drug to the back of the eye can be accomplished at very low values of current and on a short time scale and that the additional flux provided by the electric field significantly increases the drug delivery.

Absence of Damage to Posterior Eye Segment after Completion of Drug Delivery

The Nile blue imaging on a confocal microscope also revealed no apparent damage to any regions of the posterior eye

segment. It is well known that the osmotic effects can rearrange the stromal structure and reduce transparency [31,32] and similar damage may be feasible to the retina and sclera. This possibility led to the incorporation of HEPES in the lenses to mitigate these harmful side effects. We did not observe any damage which may be due to the use of the HEPES buffer or because the tissue (sclera, choroid, retina) is not as susceptible to damage from osmotic effects as the cornea.

Potential Designs for Iontophoretic Contact Lens and Electrode Arrangements

There are two potential electrode arrangements for incorporation into contact lenses. The first is concentric rings (Fig. 7a) which would have one electrode adjacent to the sclera and vitreous while the counter electrode is positioned at the just beyond or on the cornea. In this scenario, the electric field will permeate the tissue and then turn around towards the counter electrode. Diffusion in the vitreous will lead to negligible transport back into the tissue delivering drug into the vitreous. This

design would theoretically maximize the amount of drug delivery due to the large area of the electrodes while not obscuring the vision field and may even increase hydration of the cornea if the counter electrode is located at the corneal surface. The second design is one that has spot electrodes on either side of the lens and sits adjacent to the sclera (Fig. 7b). This design was the primary setup in all experiments used for delivering fluorescein and Nile Blue to the posterior eye segment. If a larger amount of drug must be delivered to the vitreous, or if axisymmetric distribution of the drug is desired in the retina, the concentric electrode arrangement may be preferred.

CONCLUSION

The results of the Nile Blue and fluorescein delivery experiments in addition to the COMSOL model suggests that efficient delivery of a drug, hydrophilic or hydrophobic, can be achieved to the posterior eye segment with our proposed

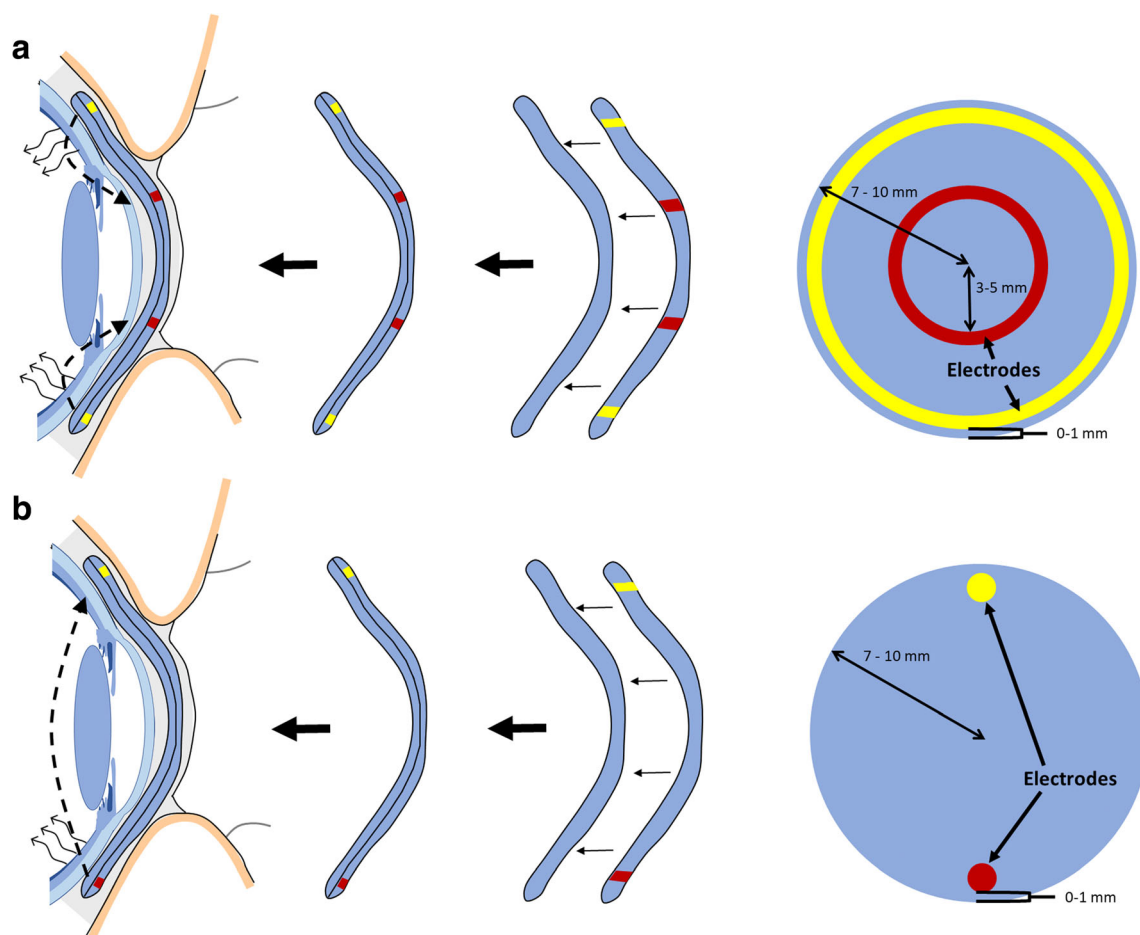


Fig. 7 Potential configurations for electrode arrangements and geometries. (a) Concentric and (b) spot electrode designs and the two-layer system for both. The lenses with electrodes will be placed on a drug loaded lens and then placed in the eye. The dashed lines indicate the primary route of the electric field as suggested by COMSOL modeling and the other arrows indicate the projected path of drug transport.

design. Although existing ocular iontophoresis studies have effectively delivered drug to their target regions, they typically employ an electrode at the ocular surface and one at the ear, causing current to pass through unwanted and sensitive regions with unknown consequences. The bulkiness and resulting discomfort of other devices also requires currents to be on the order of 1 mA or higher which is dangerously close to the threshold for cellular damage (33,34).

The system described in this study is unique regarding the compact design that would allow it to be worn like a normal contact lens and the inclusion of both electrodes on a single eye. In theory, this would improve the level of comfort and permit longer wear times that are similar to commercially available lenses. Therefore, the application time of the current can be expanded to fit that time period which results in lower necessary current values that are much safer than the existing methods. The lower current ultimately reduces the toxicity from electrochemically generated species and the potential for cell disruption. The inclusion of both electrodes on a single lens also eliminates the possibility of harmful and unforeseen consequences when current passes through other sensitive areas.

Even though efficient drug delivery through an iontophoretic contact lens has been shown to have potential, there are still three key areas of interest that require attention. The first is the complete fabrication of the entire system into a contact lens that provides sufficient current and remains consistent for long periods of time. Second, a more comprehensive and detailed computational model should be constructed. The model should include the electric field along with mass transport. Therefore, the model would have the ability to predict the required application time, the size of the electrodes, and loading concentration for drugs with different properties. Finally, a comprehensive *in vivo* study will be needed to test the safety and efficacy. We hope that these issues can be explored by researchers that are interested in delivery of drugs to the posterior eye segment while circumventing the use of intravenous injections.

REFERENCES

- Hironaka K, Inokuchi Y, Tozuka Y, Shimazawa M, Hara H, Takeuchi H. Design and evaluation of a liposomal delivery system targeting the posterior segment of the eye. *J Control Release* [Internet] Elsevier BV; 2009;136:247–253. Available from: <https://doi.org/10.1016/j.jconrel.2009.02.020>
- Geroski DH, Edelhauser HF. Transscleral drug delivery for posterior segment disease. *Adv Drug Deliv Rev*. 2001;52:37–48.
- del Amo EM, Urtti A. Current and future ophthalmic drug delivery systems. A shift to the posterior segment. *Drug Discov Today*. 2008;13:135–43.
- Patel SR, Berezovsky DE, McCarey BE, Zarnitsyn V, Edelhauser HF, Prausnitz MR. Targeted administration into the suprachoroidal space using a microneedle for drug delivery to the posterior segment of the eye. *Investig Ophthalmol Vis Sci*. 2012;53:4433–41.
- Patel A, Cholkar K, Agrahari V, Mitra AK. Ocular drug delivery systems: An overview. *World J Pharmacol*. 2015;2:47–64.
- Sasaki H, Karasawa K, Hironaka K, Tahara K, Tozuka Y, Takeuchi H. Retinal drug delivery using eyedrop preparations of poly-L-lysine-modified liposomes. *Eur J Pharm Biopharm* [Internet]. 2013;83:364–9. Available from: <https://doi.org/10.1016/j.ejpb.2012.10.014>.
- Kushwaha SK, Saxena P, Rai A. The adsorption of proteins from aqueous solution on solid surfaces. *J Control Release*. 2014;13:208–21.
- Penn JS, Madan A, Caldwell RB, Bartoli M, Caldwell RW, Hartnett ME. Vascular endothelial growth factor in eye disease. *Prog Retin Eye Res* [Internet]. NIH Public Access; 2008 [cited 2018 Oct 10];27:331–71. Available from: <http://www.ncbi.nlm.nih.gov/pubmed/18653375>. Access 10 October 2018
- Ferreira A, Sagkriotis A, Olson M, Lu J, Makin C, Milnes F. Treatment frequency and dosing interval of ranibizumab and aflibercept for neovascular age-related macular degeneration in routine clinical practice in the USA. *PLoS One*. 2015;10:1–12.
- Park SJ, Oh J, Kim YK, Park JH, Park JY, Hong HK, et al. Intraocular pharmacokinetics of intravitreal vascular endothelial growth factor-trap in a rabbit model. *Eye*. 2015;29:561–8.
- Bourlais CL, Acar L, Zia H, Sado P, Needham T, Leverage R. Ophthalmic drug delivery systems—recent advances. *Prog Retin Eye Res*. 1998;17:33–58.
- Nagarwal RC, Kumar R, Pandit JK. Chitosan coated sodium alginate-chitosan nanoparticles loaded with 5-FU for ocular delivery: In vitro characterization and in vivo study in rabbit eye. *Eur J Pharm Sci* [Internet]. Elsevier B.V.; 2012;47:678–685. Available from: <https://doi.org/10.1016/j.ejps.2012.08.008>
- Loftsson T, Hreinsdóttir D, Stefánsson E. Cyclodextrin microparticles for drug delivery to the posterior segment of the eye: aqueous dexamethasone eye drops. *Jpp*. 2007;59:629–35.
- Lee SB, Geroski DH, Prausnitz MR, Edelhauser HF. Drug delivery through the sclera: effects of thickness, hydration, and sustained release systems. *Exp Eye Res*. 2004;78:599–607.
- Münch S, Wohlrab J, Neubert RHH. Dermal and transdermal delivery of pharmaceutically relevant macromolecules. *Eur J Pharm Biopharm*. 2017;119:235–42.
- Gibson DJ, Tuli SS, Schultz GS. Dual-phase iontophoresis for the delivery of antisense oligonucleotides. *Nucleic Acid Ther*. 2017;27:238–50.
- Hao J, Li SK, Liu CY, Kao WWY. Electrically assisted delivery of macromolecules into the corneal epithelium. *Exp Eye Res Elsevier Ltd*. 2009;89:934–41.
- Patane MA, Cohen A, From S, Torkildsen G, Welch D, Ousler GW. Ocular iontophoresis of EGP-437 (dexamethasone phosphate) in dry eye patients: results of a randomized clinical trial. *Clin Ophthalmol*. 2011;5:633–43.
- Chiou J-C, Hsu S-H, Huang Y-C, Yeh G-T, Liou W-T. Wirelessly KC-KA. Powered smart contact lens with reconfigurable wide range and tunable sensitivity sensor readout circuitry. *Sensors* [Internet]. 2017;17:108 Available from: <http://www.mdpi.com/1424-8220/17/1/108>. Access 6 April 2017
- Huang YC, Yeh GT, Sen YT, Chiou JC. A contact lens sensor system with a micro-capacitor for wireless intraocular pressure monitoring. *Proc IEEE Sensors*. 2013.
- Yuvaraj AL, Santhanaraj D. A systematic study on electrolytic production of hydrogen gas by using graphite as electrode. 2014 [cited 2018 Oct 10]; Available from: <https://doi.org/10.1590/S1516-14392013005000153>
- Molokhia SA, Jeong EK, Higuchi WI, Li SK. Transscleral iontophoretic and intravitreal delivery of a macromolecule: study of

- ocular distribution in vivo and postmortem with MRI. *Exp eye res* [Internet]. Elsevier Ltd. 2009;88:418–25. Available from: <https://doi.org/10.1016/j.exer.2008.10.010>.
23. Nair AB, Goel A, Prakash S, Kumar A. Therapeutic drug monitoring by reverse iontophoresis. *J Basic Clin Pharm* [Internet] Pulsus Group; 2012 [cited 2018 Oct 10];3. Available from: <https://www.jbclinpharm.org/articles/therapeutic-drug-monitoring-by-reverse-iontophoresis.html>. Access 10 October 2018
 24. Georges JM. Microscopic aspects of adhesion and lubrication [Internet]. Elsevier Scientific Pub. Co.; 1982 [cited 2018 Oct 11]. Available from: <https://books.google.com/books?id=aqMqqj9KxL0C&pg=PA127&lpg=PA127&dq=%22nile+blue%22+pka+source=b1&ots=0VhF15KqBb&sig=8ibY7LcWRacvEbVzD5vr83Yttjk&hl=en&sa=X&ved=2ahUKEwj-vbrZ0f7dAhWxq4MKHc9cCwQQ6AEwBH0ECAIQAQ#v=onepage&q=%22nileblue%22pka&f=false>. Access 11 October 2018
 25. Cruysberg LPJ, Nuijts RMMA, Geroski DH, Koole LH, Hendrikse F, Edelhauser HF. *In Vitro* human scleral permeability of fluorescein, dexamethasone-fluorescein, methotrexate-fluorescein and rhodamine 6G and the use of a coated coil as a new drug delivery system. *J Ocul Pharmacol Ther* [Internet] 2002;18:559–569. Available from: <https://doi.org/10.1089/108076802321021108>. Access 11 April 2018
 26. Jackson TL, Hussain A, Morley AMS, Sullivan PM, Hodgetts A, El-Osta A, et al. Scleral hydraulic conductivity and macromolecular diffusion in patients with uveal effusion syndrome. *Investig Ophthalmol Vis Sci*. 2008;49:5033–40.
 27. Balachandran RK, Barocas VH. Computer modeling of drug delivery to the posterior eye : effect of active transport and loss to choroidal blood flow. *Pharm Res*. 2008;25:2685–96.
 28. Vollmer DL, Lloyd LB, Szlek MA, Kolb K, Parkinson TM. In vivo Transscleral iontophoresis of amikacin to rabbit eyes. *J Ocul Pharmacol Ther*. 2003;18:549–58.
 29. Palestine AG, Brubaker RF. Pharmacokinetics of fluorescein in the vitreous. *Investig Ophthalmol Vis Sci*. 1981;21:542–9.
 30. Bakri SJ, Snyder MR, Reid JM, Pulido JS, Ezzat MK, Singh RJ. Pharmacokinetics of Intravitreal Ranibizumab (Lucentis). *Ophthalmology* [Internet]. Elsevier; 2007 [cited 2019 Feb 19];114:2179–82. Available from: <https://www.sciencedirect.com/science/article/pii/S0161642007010305>
 31. Kostyuk O, Nalovina O, Mubard TM, Regini JW, Meek KM, Quantock AJ, et al. Transparency of the bovine corneal stroma at physiological hydration and its dependence on concentration of the ambient anion. *J Physiol*. 2002;543:633–42.
 32. Meek KM, Knupp C. Corneal structure and transparency. *Prog Retin Eye Res* Elsevier Ltd. 2015;49:1–16.
 33. Frucht-Pery J, Mechoulam H, Siganos CS, Ever-Hadani P, Shapiro M, Domb A. Iontophoresis-gentamicin delivery into the rabbit cornea, using a hydrogel delivery probe. [cited 2018 Oct 10]; Available from: www.elsevier.com/locate/yexer, 2004
 34. Eljarrat-Binstock E, Raikup F, Stepensky D, Domb AJ, Frucht-Pery J. Delivery of gentamicin to the rabbit eye by drug-loaded hydrogel iontophoresis. *Investig Ophthalmol Vis Sci*. 2004;45:2543–8.
 35. Zhao M, Chalmers L, Cao L, Vieira AC, Mannis M, Reid B. Electrical signaling in control of ocular cell behaviors. *Prog Retin Eye Res*. 2012;31:65–88.
 36. Minnikanti S, Cohen E, Peixoto N. Quasi-static analysis of electric field distributions by disc electrodes in a rabbit eye model. *IFMBE Proc*. 2010;32:385–8.
 37. Brindley GS. The passive electrical properties of the frog's retina, choroid and sclera for radial fields and currents. *J Physiol*. 1956;134:339–52.
 38. Reinach PS, Podos SM. *Electrical Measurements Rabbit Iris-Ciliary Body on the Isolated*. 1984.

Publisher's Note Springer Nature remains neutral with regard to jurisdictional claims in published maps and institutional affiliations.